Analysis of a multistable dynamical system describing a competitive interaction between synapses on a neuron

Hiroshi Okamoto and Kazuhisa Ichikawa
Foundation Research Laboratory, Fuji Xerox Company Ltd., Kanagawa 243-04, Japan
(Received 20 September 1993)

Recently, Lisman proposed an attractive idea that a use-dependent change in the strength of transmission efficiency at a synapse, thought of as an elementary process of learning and memory in the brain, is attributed to the switching of biochemical activity. He postulated two enzymes in a postsynaptic spine: One undergoes autocatalytic activation; the other deactivates the active form of the former enzyme. He showed that these enzymatic reactions yield two distinct thermal equilibrium limits and the total system functions as a bistable switch. In the original Lisman model, these enzymatic reactions are considered to be closed in each spine. In this paper, we generalize his model by taking solubilities of the enzymes into account, and discuss what kind of interaction between the modification processes at neighboring synapses formed on the same neuron is caused by cytosolic enzyme transportation between spines. Our model is described by a nonlinear dynamical system whose structure we investigate in analytical and numerical ways. Results show that this system can be multistable and exhibit spontaneous symmetry breaking, which represents a competitive interaction between the modification processes. This interaction leads to a phenomenon which has been dubbed "synapse selection:" The weight of only one of the synapses, which is the strongest at an initial time, is selected and enhanced, and those of the others are returned to their basal levels with time in ascending order of their initial strengths. In addition, a difficulty associated with the original Lisman model, that the parameter range which allows the system to function as a switch is relatively narrow and accordingly the switch mechanism is functionally unstable against small changes in parameters, is considerably improved in our generalized scheme by broadening the parameter range. In this broadened parameter range, the system works as a hybridized switch, i.e., a switch with the function of synapse selection.

PACS number(s): 87.10.+e, 87.22.Jb, 87.22.Me

I. INTRODUCTION

Processing of information in the brain is carried out by signal transmissions in neural networks. A locus through which signals are transferred from one neuron to the next is called a *synapse*. It is a widely accepted idea that a use-dependent change in the strength of transmission efficiency at a synapse (synaptic weight) is an elementary process of learning and memory [1].

Recently, Lisman [2] proposed a bistable molecular switch as a possible model for such a synaptic-modification process. He postulated two enzymes in a postsynaptic spine: One undergoes activation of itself, i.e., autocatalytic activation, and the active form of this enzyme is responsible for synaptic enhancement; the other undergoes inactivation of the active form of the former enzyme. In this paper, the former and the latter enzymes will be referred to as an *enhancer* and an *inactivator*, respectively. It was shown that autocatalytic activation of the enhancer *versus* its inactivation can yield two distinct thermal equilibrium states: In one state, a portion of the enhancer in a spine is in the active form, and hence, the synaptic weight is at an enhanced level, that is, the molecular switch is "ON;" in the other state, all of the enhancer in the spine is in the inactive form and, hence, the synaptic weight is at its basal level, that is, the molecular switch is "OFF."

The enhancer in a spine is activated through either of the following two processes: (1) It is activated when a signal is transferred from a presynaptic terminal to a postsynaptic spine; (2) it is also activated through autocatalysis, as mentioned above. Suppose that all of the enhancer in a spine is in the inactive form at an initial time, namely, the molecular switch is OFF. Then, a signal transmission takes place, and, as a result, a quantity of the enhancer, proportional to the intensity of the signal, is activated through process (1) as well as through process (2). The signal transmission and resulting activation of the enhancer through process (1) are transient. After termination of them, nevertheless, autocatalytic activation of the enhancer [process (2)] still continues. There is a threshold with respect to the concentration of the active enhancer: If the intensity of the signal is strong enough to raise the concentration of the active enhancer above this threshold, then the molecular switch is turned ON.

Lisman's scheme was proposed as a hypothetical one; it has not yet been verified by experiment. Indeed, molecular mechanisms of synaptic-modification processes are far from established [3]. In spite of that, a use-dependent switching of biochemical activity responsible for synaptic enhancement is one of the most plausible and also one of the most attractive ideas that can theoretically explain a molecular mechanism underlying a synaptic-modification process. Therefore, one can employ Lisman's model as a molecular-mechanical basis for a further discussion of general properties of a synaptic-modification process.

Molecular mechanisms of synaptic-modification processes in the real brain may be much more complicated than that proposed by Lisman, but his model probably represents some essential features of them.

In a real neuron, a lot of synapses are formed on somas and dendrites at high density [4]. In Lisman's model, nevertheless, the enzymatic reactions are considered to be a closed system confined to each spine, and hence the molecular switch at each spine functions independently of those at others. This, however, is no longer the case if the enzymes are soluble because soluble enzymes cannot be confined to each spine permanently, but can leak out from a spine, diffuse in cytosol, and enter another spine. This eventually causes some kind of interaction between the modification processes at neighboring synapses formed on the same neuron. In other words, the molecular switch at each spine can no longer function independently of those at others. In fact, there are numerous enzymes in cells, and some of them are soluble in cytosol while others are insoluble—more precisely, associated to membrane. Furthermore, there are also not a small number of enzymes that are soluble or membrane associated in one form, but change their solubilities in another form.

In this paper we will generalize the original Lisman model, taking solubilities of the enzymes into account, and discuss how the modification processes at synapses on a neuron interact with one another via cytosolic enzyme transportation between spines. Investigation of such a cellular level of phenomenon is also significant from the viewpoint of information processing in neural networks; cooperativity or competition between synapses caused by such an interaction must be implicated in pattern encoding in neuronal connections, and thereby has considerable influence upon network levels of information processing. Our generalized scheme appears to be described by a nonlinear dynamical system. We will therefore investigate the dynamical behavior of our model by analyzing the mathematical structure of this nonlinear dynamical system. A preliminary report of this work has been presented in [5].

II. CONSTRUCTION OF A MODEL

Lisman postulated typical enzymatic reactions in the following scheme as a closed system in a postsynaptic spine [2]:

$$E^*+E \underset{k_{-1}}{\overset{k_1}{\rightleftarrows}} E^*E \xrightarrow{k_2} E^*+E^* , \tag{2.1}$$

$$I+E^* \underset{k_{-3}}{\overset{k_3}{\rightleftarrows}} IE^* \xrightarrow{k_4} I+E . \tag{2.2}$$

Here, E and E^* symbolize the enhancer in the active form and that in the inactive form, respectively, and I symbolizes the inactivator. The designations k_1, k_{-1}, k_2, k_3, k_{-3}, and k_4 are rate constants. Reaction (2.1) describes autocatalytic activation of the enhancer: A molecule of the enhancer in the active form catalyzes the activation of another molecule of the enhancer in the inactive form. Reaction (2.2) describes inactivation of the enhancer in the active form.

Now we will generalize the original Lisman model, taking solubilities of the enzymes into account. In this paper we assume that E is soluble, whereas the enhancer and the inactivator in the other forms are membrane associated, that is, E is transported in cytosol by diffusion from one spine to another, whereas the enhancer and the inactivator in the other forms are confined to each spine. Of course, one can consider other situations, but we do not deal with them in this paper (see Sec. IV). A schematic drawing of our model is given in Fig. 1.

Cytosolic transportation of E from the jth spine to the ith one is represented by flow flux in the form

$$J_{E_{ij}} = -\frac{D_E S([E]_i - [E]_j)}{Vd} , \tag{2.3}$$

where D_E is the diffusion constant for E; V, S, and d are the volume of each spine, the area of its mouth, and distance between two spines, respectively; $[E]_i$ is the concentration of E in the ith spine; and $i,j=1,\ldots,N$, with N being the number of neighboring synapses interacting with one another through cytosolic transportation of E. For mathematical simplicity, V, S, and d are assumed to be constant with i (and j).

Consider a group of neighboring spines formed on the same neuronal-cell membrane and suppose that in each spine all portions of the enhancer are in the inactive form at an initial time. Then, signals are transferred through synapses; each signal transmission occurs transiently and synchronously to the others. In each spine, in turn, a quantity of the enhancer, proportional to the intensity of the signal, is then activated. It is therefore natural to define the intensity of the signal transferred through the ith synapse by the initial value of $[E^*]_i$, the concentration of the active enhancer in the ith spine.

Let $[E^*]_i$, $[E^*E]_i$, $[IE^*]_i$, and $[I]_i$ be the concentrations of E^*, E^*E, IE^*, and I in the ith spine, respectively. After the termination of the signal transmissions, the time evolution of the concentrations of the enzymes in the ith spine is then described by the following equations [6]:

$$\frac{d[E^*]_i}{dt} = -k_1[E]_i[E^*]_i + (k_{-1}+2k_2)[E^*E]_i - k_3[E^*]_i[I]_i + k_{-3}[IE^*]_i , \tag{2.4}$$

$$\frac{d[E]_i}{dt} = -k_1[E]_i[E^*]_i + k_{-1}[E^*E]_i + k_4[IE^*]_i + \sum_{j=1}^{N} J_{E_{ij}} , \tag{2.5}$$

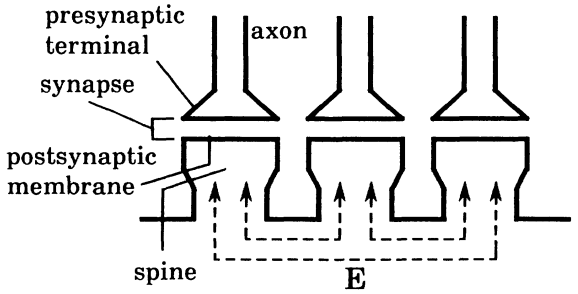

FIG. 1. Schematic drawing of our model.

$$\frac{d[E^*E]_i}{dt}=k_1[E]_i[E^*]_i-(k_{-1}+k_2)[E^*E]_i\ , \tag{2.6}$$

$$\frac{d[I]_i}{dt}=-k_3[E^*]_i[I]_i+(k_{-3}+k_4)[IE^*]_i\ , \tag{2.7}$$

$$\frac{d[IE^*]_i}{dt}=k_3[E^*]_i[I]_i-(k_{-3}+k_4)[IE^*]_i\ . \tag{2.8}$$

From (2.4)–(2.8) one finds that

$$\sum_{i=1}^{N}([E]_i+[E^*]_i+2[E^*E]_i+[IE^*]_i)$$

and $[I]_i+[IE^*]_i$ are held constant with time. Further assuming that $[I]_i+[IE^*]_i$ is also constant with i, one can set

$$\sum_{i=1}^{N}([E]_i+[E^*]_i+2[E^*E]_i+[IE^*]_i)=NC_E \tag{2.9}$$

and

$$[I]_i+[IE^*]_i=C_I\quad(i=1,\ldots,N)\ , \tag{2.10}$$

where C_E and C_I are constants. Equations (2.9) and (2.10) represent conservation laws for the enhancer and the inactivator, respectively.

Lisman [2] postulated steady-state assumptions [7] for the intermediary metabolites, E^*E and IE^*. These assumptions greatly simplified the scheme, reducing the number of variables and parameters without spoiling the essential features of the model. Following Lisman, we also postulate steady-state assumptions, as follows:

$$\frac{d[E^*E]_i}{dt}=0\ , \tag{2.11}$$

$$\frac{d[IE^*]_i}{dt}=0\ , \tag{2.12}$$

for $i=1,\ldots,N$. On the basis of these assumptions, one can substitute the following simplified equations for the original ones:

$$\frac{d[E^*]_i}{dt}=\frac{k_2[E]_i[E^*]_i}{K_A}-\frac{V_I[E^*]_i}{[E^*]_i+K_I}\ , \tag{2.13}$$

$$\frac{d[E^*]_i}{dt}=-\frac{k_2[E]_i[E^*]_i}{K_A}+\frac{V_I[E^*]_i}{[E^*]_i+K_I}+\sum_{j=1}^{N}J_{E_{ij}}\ , \tag{2.14}$$

$$\sum_{i=1}^{N}([E]_i+[E^*]_i)=N\bar{C}_E\ , \tag{2.15}$$

where $\bar{C}_E$ is defined by

$$\bar{C}_E=C_E-\frac{1}{N}\sum_{i=1}^{N}(2[E^*E]_i+[IE^*]_i)\ , \tag{2.16}$$

which is a constant because $[E^*E]_i$ and $[IE^*]_i$ are held constant with time [see (2.11) and (2.12)]. In (2.13) and (2.14), K_A and K_I are Michaelis constants [7] for reactions (2.1) and (2.2), respectively, and V_I is maximal velocity [7] for reaction (2.2); they are defined by

$$K_A=\frac{k_{-1}+k_2}{k_1}\ , \tag{2.17}$$

$$K_I=\frac{k_{-3}+k_4}{k_3}\ , \tag{2.18}$$

$$V_I=k_4C_I\ . \tag{2.19}$$

For convenience for later discussion, we rewrite (2.13)–(2.15) into dimensionless forms as

$$\frac{dx_i}{ds}=\frac{x_iy_i}{\beta}-\frac{x_i}{x_i+\gamma}\ , \tag{2.20}$$

$$\frac{dy_i}{ds}=-\frac{x_iy_i}{\beta}+\frac{x_i}{x_i+\gamma}+\delta\left[\sum_{j=1}^{N}y_j-Ny_i\right]\ , \tag{2.21}$$

$$\sum_{i=1}^{N}(x_i+y_i)=N\alpha\ , \tag{2.22}$$

where x_i, y_i, α, β, γ, and δ are dimensionless variables and parameters defined by

$$x_i=\frac{k_2}{V_I}[E^*]_i\ , \tag{2.23}$$

$$y_i=\frac{k_2}{V_I}[E]_i\ , \tag{2.24}$$

$$s=k_2t\ , \tag{2.25}$$

$$\alpha=\frac{k_2}{V_I}\bar{C}_E\ , \tag{2.26}$$

$$\beta=\frac{k_2}{V_I}K_A\ , \tag{2.27}$$

$$\gamma=\frac{k_2}{V_I}K_I\ , \tag{2.28}$$

$$\delta=\frac{D_ES}{k_2Vd}\ . \tag{2.29}$$

III. ANALYTICAL AND NUMERICAL INVESTIGATION OF THE MODEL

Our problem is now described by the nonlinear dynamical system (2.20)–(2.22). This system gives trajectories of the state point P whose coordinate representation is (x_i,y_i). The trajectories are constrained on the $(2N-1)$-dimensional hyperplane (2.22) embedded in the $2N$-dimensional phase space. The dynamical behavior of our model can therefore be understood by investigating the mathematical structure of these trajectories. To do this, we will first determine stabilities of equilibrium points of this system as functions of the parameters.

With the definitions

$$F_i=\frac{x_iy_i}{\beta}-\frac{x_i}{x_i+\gamma}\ , \tag{3.1}$$

$$G_i=-\frac{x_iy_i}{\beta}+\frac{x_i}{x_i+\gamma}+\delta\left[\sum_{j=1}^{N}y_j-Ny_i\right]\ , \tag{3.2}$$

(2.20) and (2.21) become

$$\dot{x}_i = F_i \ , \tag{3.3}$$

$$\dot{y}_i = G_i \ , \tag{3.4}$$

where a dot above a variable means d/ds. The coordinates of equilibrium points of the system are given as positive roots of the algebraic equations

$$F_i = G_i = 0 \ , \tag{3.5}$$

simultaneously with (2.22). Defining parameters μ and ν by

$$\mu = \beta - \alpha\gamma \ , \tag{3.6}$$

$$\nu = \frac{N[2\beta - \alpha\gamma - 2\sqrt{\beta(\beta-\alpha\gamma)}]}{\gamma^2} \ , \tag{3.7}$$

we can easily prove that (i) when

$$\mu < 0 \ , \tag{3.8}$$

equilibrium points of the system are listed as P_0 and P_{L_n} $(n = 1, \ldots, N)$; (ii) when

$$\mu > 0 \quad \text{and} \quad \nu > 1 \ , \tag{3.9}$$

equilibrium points of the system are listed as P_0, P_{L_n} $(n = 1, \ldots, n_M)$, and P_{S_n} $(n = 1, \ldots, n_M)$; and (iii) when

$$\mu > 0 \quad \text{and} \quad \nu < 1 \ , \tag{3.10}$$

the system has only one equilibrium point, P_0. In (i)–(iii), P_0, P_{L_n}, and P_{S_n} are state points whose coordinates satisfy

$$x_1 = \cdots = x_N = 0 \ , \quad y_1 = \cdots = y_N = \alpha \ , \tag{3.11}$$

$$x_{k_1} = \cdots x_{k_n} = v_{L_n} \ , \quad x_{k_{n+1}} = \cdots = x_{k_N} = 0 \ ,$$

$$y_1 = \cdots = y_N = \frac{\beta}{v_{L_n} + \gamma} \ , \tag{3.12}$$

and

$$x_{k_1} = \cdots x_{k_n} = v_{S_n} \ , \quad x_{k_{n+1}} = \cdots = x_{k_N} = 0 \ ,$$

$$y_1 = \cdots = y_N = \frac{\beta}{v_{S_n} + \gamma} \ , \tag{3.13}$$

respectively; n is an integer satisfying $1 \le n \le N$, $(k_1, \ldots, k_N)$ is an arbitrary permutation of $(1, \ldots, N)$, and v_{L_n} and v_{S_n} are larger and smaller roots of the quadratic equation

$$nv^2 - (N\alpha - n\gamma)v + N(\beta - \alpha\gamma) = 0 \ . \tag{3.14}$$

respectively; n_M is the maximum of n's that satisfy

$$N\alpha - n\gamma > 0, \quad (N\alpha - n\gamma)^2 - 4nN(\beta - \alpha\gamma) > 0 \ . \tag{3.15}$$

Stabilities of these equilibrium points will be determined using standard procedures in the linearized theory [8], as below. Let $(x_i^{(\mathrm{eq})}, y_i^{(\mathrm{eq})})$ be the coordinate representation of an equilibrium point, $P^{(\mathrm{eq})}$, and consider small-perturbed trajectories around it:

$$x_i = x_i^{(\mathrm{eq})} + \chi_i \ , \tag{3.16}$$

$$y_i = y_i^{(\mathrm{eq})} + \psi_i \ , \tag{3.17}$$

where χ_i and ψ_i are small quantities. A given equilibrium point is (asymptotically) stable if $\chi_i \to 0$ and $\psi_i \to 0$ as $s \to \infty$. Substituting (3.16) and (3.17) into (3.3) and (3.4), expanding their right-hand side terms into Taylor series with respect to χ_i and ψ_i, and neglecting quadratic and higher-order terms, we obtain

$$\dot{\chi}_i = \sum_{j=1}^{N} \left. \frac{\partial F_i}{\partial \chi_j} \right|_{\chi=\psi=0} \chi_j + \sum_{j=1}^{N} \left. \frac{\partial F_i}{\partial \psi_j} \right|_{\chi=\psi=0} \psi_j \ , \tag{3.18}$$

$$\dot{\psi}_i = \sum_{j=1}^{N} \left. \frac{\partial G_i}{\partial \chi_j} \right|_{\chi=\psi=0} \chi_j + \sum_{j=1}^{N} \left. \frac{\partial G_i}{\partial \psi_j} \right|_{\chi=\psi=0} \psi_j \ . \tag{3.19}$$

Introducing a $2n \times 2n$ matrix A and a $2n$-dimensional column vector ξ defined by

$$A = \begin{bmatrix} \left. \frac{\partial F_i}{\partial \chi_j} \right| & \left. \frac{\partial F_i}{\partial \psi_j} \right| \\ \left. \frac{\partial G_i}{\partial \chi_j} \right| & \left. \frac{\partial G_i}{\partial \psi_j} \right| \end{bmatrix} \ , \tag{3.20}$$

$$\xi = \begin{bmatrix} \chi_i \\ \psi_i \end{bmatrix} \ , \tag{3.21}$$

the set of (3.18) and (3.19) acquires the form

$$\dot{\xi} = A\xi \ . \tag{3.22}$$

These linear differential equations can be solved by the hypothesis

$$\xi = \xi_0 \exp(\lambda t) \ . \tag{3.23}$$

Here λ is a root of the algebraic equation

$$|A - \lambda I| = 0 \ , \tag{3.24}$$

where I is the $2n \times 2n$ unit matrix.

When $P^{(\mathrm{eq})} = P_0$, Eq. (3.24) is evaluated as

$$\lambda(\lambda + N\delta)^{N-1} \left[\lambda + \frac{\beta - \alpha\gamma}{\beta\gamma} \right]^N = 0 \ ; \tag{3.25}$$

when $P^{(\mathrm{eq})} = P_{L_n} (v = v_{L_n})$ or $P^{(\mathrm{eq})} = P_{S_n} (v = v_{S_n})$, (3.24) becomes

$$\lambda(\lambda + N\delta)^{N-n-1} \left[\lambda + \frac{v}{(v+\gamma)\gamma} \right]^{N-n} \left[\lambda^2 - \left[N\delta + \frac{v}{\beta} + \frac{v}{(v+\gamma)^2} \right] \lambda + \frac{N\delta v}{(v+\gamma)^2} \right]^{n-1}$$

$$\times \left[\lambda^2 + \left[N\delta + \frac{v}{\beta} - \frac{v}{(v+\gamma)^2} \right] \lambda + \delta \left[\frac{nv}{\beta} - \frac{Nv}{(v+\gamma)^2} \right] \right] = 0 \ . \tag{3.26}$$

Both (3.25) and (3.26) have a root $\lambda=0$, which reflects the conservation law (2.22). The mode corresponding to this root represents translations vertical to the hyperplane (2.22). If the real parts of all the other λ's are negative, the given equilibrium point, which is on this hyperplane, is stable against small perturbations horizontal to this hyperplane. If any one of them is positive, the equilibrium point is unstable.

If $\mu>0$, then all the roots of (3.25) except $\lambda=0$ are negative; if $\mu<0$, then (3.25) has an n-multiple positive root, $-(\beta-\alpha\gamma)/\beta\gamma$. Therefore, P_0 is stable if $\mu>0$, and it is unstable if $\mu<0$.

Critical factors in (3.26), which are responsible for stabilities of either P_{L_n} or P_{S_n}, are

$$\lambda^2-\left[N\delta+\frac{v}{\beta}+\frac{v}{(v+\gamma)^2}\right]\lambda+\frac{N\delta v}{(v+\gamma)^2}$$

and

$$\lambda^2+\left[N\delta+\frac{v}{\beta}-\frac{v}{(v+\gamma)^2}\right]\lambda+\delta\left[\frac{nv}{\beta}-\frac{Nv}{(v+\gamma)^2}\right].$$

Consider, therefore, the following quadratic equations:

$$\lambda^2-\left[N\delta+\frac{v}{\beta}+\frac{v}{(v+\gamma)^2}\right]\lambda+\frac{N\delta v}{(v+\gamma)^2}=0\,, \tag{3.27}$$

$$\lambda^2+\left[N\delta+\frac{v}{\beta}-\frac{v}{(v+\gamma)^2}\right]\lambda+\delta\left[\frac{nv}{\beta}-\frac{Nv}{(v+\gamma)^2}\right]=0\,. \tag{3.28}$$

Both of the roots of (3.27) are positive. They are also roots of (3.26) except when $n=1$. When $v=v_{L_n}$, (3.28) has two negative roots if $\mu<0$ or if $\mu>0$ and $\nu>1$. Therefore, P_{L_n} is stable only when $n=1$. When $v=v_{S_n}$, (3.28) has one positive and one negative root if $\mu>0$ and $\nu>1$. Therefore, P_{S_n} is unstable.

Results in the above discussion are summarized in Table I. As seen in this table, the parameter space is divided into three regions according to equilibrium points and their stabilities, as follows.

(i) When $\mu>0$, the system has only one kind of stable focus, P_{L_1}, which is N multiplicated as

$$(x_1,x_2,x_3,\ldots,x_{N-1},x_N)=(v_{L_1},0,0,\ldots,0,0),(0,v_{L_1},0,\ldots,0,0),\ldots,(0,0,0,\ldots,0,v_{L_1})\,.$$

The system is therefore N multistable.

(ii) When $\mu>0$ and $\nu>1$, the system has two kinds of stable focuses, P_0 and P_{L_1}. The system is therefore $N+1$ multistable.

(iii) When $\mu>0$ and $\nu<1$, the system has only one stable focus, P_0, and hence the system is monostable.

Note also that all λ's that satisfy (3.25) or (3.26) are real. From this and the above findings, one can expect that limit cycles or chaotic behavior do not occur, and the state point is always attracted to either P_0 or P_{L_1} as $s\to\infty$. To verify this expectation, we performed numerical simulations of the time evolution of the system under each of the following conditions: (i) $\mu<0$; (ii) $\mu>0$ and $\nu>1$; (iii) $\mu>0$ and $\nu<1$. In these simulations, we postulated an idealized situation that x_i+y_i, which is proportional to the total of active- and inactive-enhancer concentrations, is constant with i at an initial time. With (2.22), we have thereby the following initial conditions:

$$0<x_i<\alpha\,, \tag{3.29}$$

$$y_i=\alpha-x_i\,, \tag{3.30}$$

for $i=1,\ldots,N$ at $s=0$. As stated previously, the initial value of $[E^*]_i$, or equivalently, that of x_i [see (2.23)] defines the intensity of signal transmission at the ith synapse. If the initial values of x_i's satisfy $x_1>x_2>\cdots>x_N$, we always obtained results like those shown in Fig. 2. The results indicate that (i) when $\mu<0$, P, the state point, is attracted to P_{L_1} as $s\to\infty$ regardless of the initial values of x_i's [Fig. 2(a)]; (ii) when $\mu>0$ and $\nu>1$, P is attracted to either P_0 or P_{L_1} [Figs. 2(b) and 2(c)], i.e., the system has two kinds of thermal equilibri-

TABLE I. Equilibrium points of the nonlinear dynamical system (2.20)–(2.22) and their stabilities. S and U represent stable and unstable, respectively.

		Equilibrium points	Stability	
$\mu>0$		P_0	U	(i)
		P_{L_1}	S	
		P_{L_n} $(n=2,\ldots,N)$	U	
$\mu<0$	$\nu>1$	P_0	S	(ii)
		P_{L_1}	S	
		P_{L_n} $(n=2,\ldots,n_M)$	U	
		P_{S_n} $(n=1,\ldots,n_M)$	U	
	$\nu<1$	P_0	S	(iii)

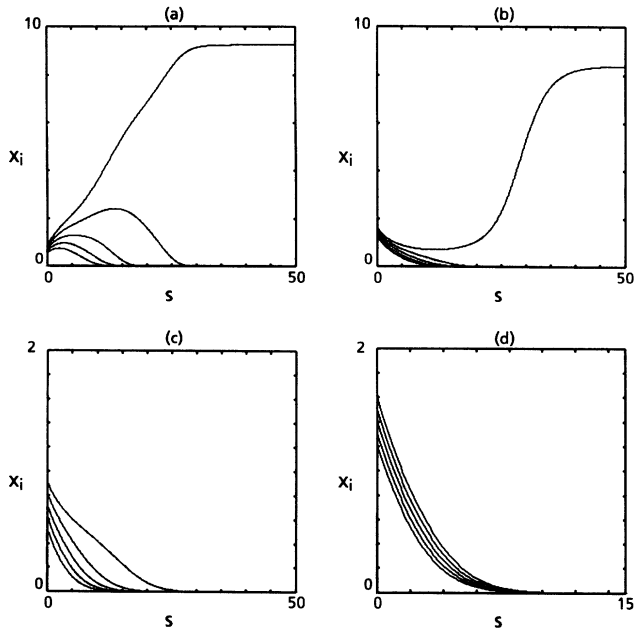

FIG. 2. Time evolutions of x_i's for $N=5$. The parameter values and the initial conditions are set for each figure, as follows: In (a) $(\alpha,\beta,\gamma,\delta)=(2.0,1.5,1.0,1.0)$ and $(x_1,x_2,x_3,x_4,x_5)_{s=0}=(1.0,0.9,0.8,0.7,0.6)$; in (b) and (c) $(\alpha,\beta,\gamma,\delta)=(2.0,1.5,1.0,1.0)$, and $(x_1,x_2,x_3,x_4,x_5)_{s=0}$ is (1.6,1.5, 1.4, 1.3, 1.2) and (0.9,0.8,0.7,0.6,0.5) in (d) and (c), respectively; and in (d) $(\alpha,\beta,\gamma,\delta)=(2.0,7.0,1.0,1.0)$, and $(x_1,x_2,x_3,x_4,x_5)_{s=0}=(1.6,1.5,1.4,1.3,1.2)$.

um states; and (iii) when $\mu>0$ and $\nu<1$, P is attracted to P_0 regardless of the initial values of x_i's [Fig. 2(d)].

It is worthwhile to visualize the structure of trajectories in the phase space. To demonstrate this, we have chosen the simplest case $N=2$ and numerically calculated the orthogonal projections of trajectories onto the x_1x_2 plane. Since (3.29) and (3.30) for $N=2$ define a two-dimensional regular square embedded in the four-dimensional phase space and each point in this regular square uniquely defines a trajectory starting from it, we picked up various points covering the entire region of this regular square as initial ends of trajectories. Results of the calculations, which are presented in Fig. 3, are as follows.

(i) When $\mu<0$, the difference between x_1 and x_2 at $s=0$, even if it is extremely small, is amplified with time, and as a result, $P_\perp$, the orthogonal projection of P onto the x_1x_2 plane, converges to $(v_{L_1},0)$ [Fig. 3(a)].

(ii) When $\mu>0$ and $\nu>1$, if both x_1 and x_2 are small enough at $s=0$ or if the difference between them is small at $s=0$ even though x_1 and x_2 themselves are not so small, then $P_\perp\rightarrow(0,0)$ [Fig. 3(b)]. Otherwise, $P_\perp\rightarrow(v_{L_1},0)$ [Fig. 3(b)]. Thus, there are thresholdlike boundaries in the x_1x_2 plane (Fig. 4), and therefore the system functions as a switch: If $P_\perp$ starts from the shaded region in Fig. 4, then the switch is turned OFF; otherwise (the open region in Fig. 4), it is turned ON.

(iii) When $\mu>0$ and $\nu<1$, $P_\perp$ always converges to (0,0) [Fig. 3(c)].

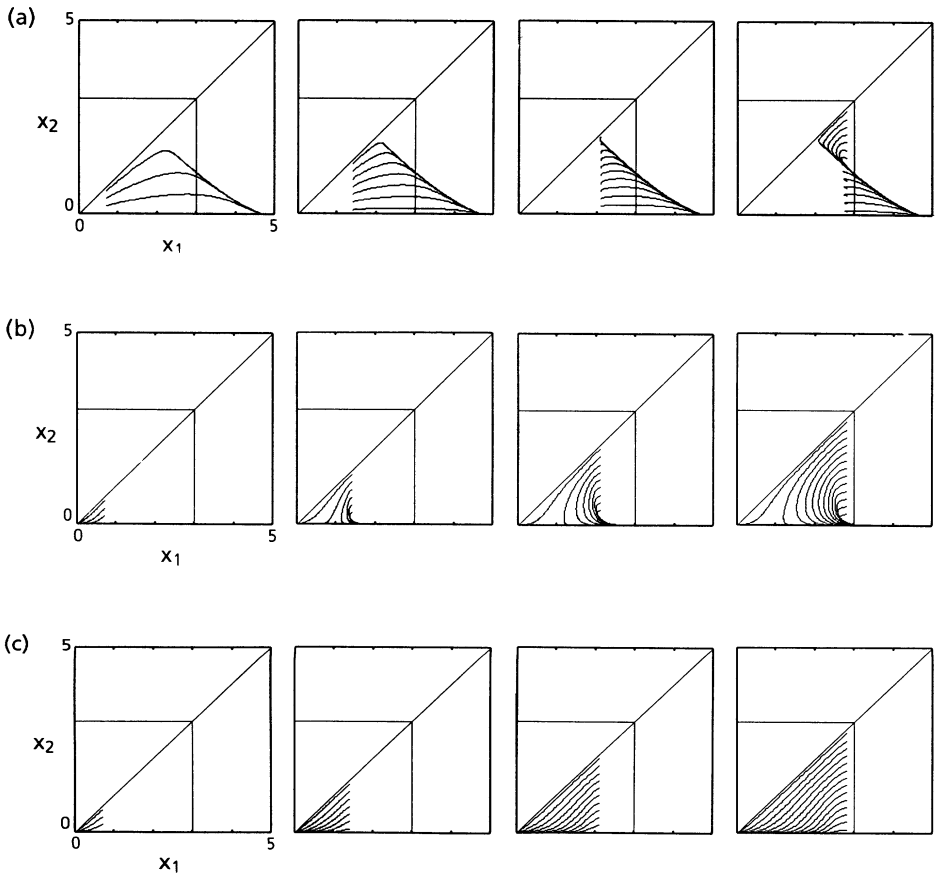

FIG. 3. Orthogonal projections of trajectories onto the x_1x_2 plane for $N=2$. The parameter values and the initial conditions are set for each figure, as follows: In (a), $(\alpha,\beta,\gamma,\delta)=(3.0,5.0,3.0,1.0)$; in (b), $(\alpha,\beta,\gamma,\delta)=(3.0,5.0,1.0,1.0)$; and in (c), $(\alpha,\beta,\gamma,\delta)=(3.0,7.0,1.0,1.0)$. Various points in the regular square defined by (3.29) and (3.30) were picked up as the initial ends of trajectories so that they cover the entire region of this regular square. The final end of each trajectory is $(v_{L_1},0)$ in (a) $(v_{L_1},0)$ or (0,0) in (b), and (0,0) in (c). The value of v_{L_1} is 4.70... and 4.0 in (a) and (b), respectively.

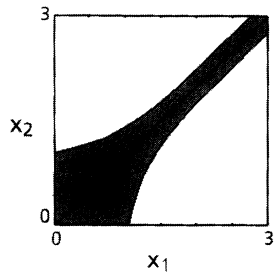

FIG. 4. Relation between $(x_1,x_2)_{s=0}$ and the final state of the switch. The parameter values were set as the same as those for Fig. 3(b). If (x_1,x_2) starts from the shaded region, then the switch is turned OFF; if it starts from either of the open regions, then the switch is turned ON.

Notice that the mathematical scheme (2.20)–(2.22) is symmetric with respect to the change $(x_i,y_i)\leftrightarrow(x_j,y_j)$ with i and j being arbitrary integers satisfying $1\le i\le N$ and $1\le j\le N$. On the other hand, Table I indicates that this symmetry can be spontaneously broken by the physically realized asymmetric state P_{L_1}, in which one of the x_i's is positive, whereas the others are zero. Figures 2(a) and 2(b) further indicate that, among the x_i's, the one that is the largest at an initial time converges to a positive value, whereas the other decay to zero with time in ascending order of their initial values. As mentioned before, x_i is a dimensionless variable that is proportional to $[E^*]_i$ [see (2.23)] and the weight of the ith synapse is a monotonic increasing function of $[E^*]_i$. Therefore, spontaneous symmetry breaking in the above represents a competitive interaction between the modification processes of the weights of synapses on a neuron, resulting in a novel phenomenon which has been dubbed "synapse selection": The weight of one of the synapses, which is the largest at an initial time, is selectively enhanced, and those at the others are returned to their basal levels in ascending order of their initial strengths.

Our generalized scheme offers an additional improvement: The original Lisman model is associated with a difficulty of functional instability of the switch mechanism [2]; this difficulty, however, is dramatically solved in our generalized scheme, as below. We have shown for $N=2$ that the system functions as a switch when the condition (3.9) is satisfied [Figs. 3(b) and 4]; this result may be generalized for $N>2$. We rewrite the condition (3.9) here again in terms of α, β, and γ:

$$\beta-\alpha\gamma>0 \quad \text{and} \quad \frac{N[2\beta-\alpha\gamma-2\sqrt{\beta(\beta-\alpha\gamma)}]}{\gamma^2}>1 \ . \tag{3.31}$$

The condition under which the original Lisman model functions as a switch is simply obtained by setting $N=1$ in (3.31), as

$$\beta-\alpha\gamma>0 \quad \text{and} \quad \frac{2\beta-\alpha\gamma-2\sqrt{\beta(\beta-\alpha\gamma)}}{\gamma^2}>1 \ . \tag{3.32}$$

A problem in the original Lisman model is the following: The parameter range defined by (3.32) is relatively narrow, so that we must finely tune the parameter values so as to make the system function as a switch. In other words, the switch mechanism in the original Lisman model is very delicate against small changes in biochemical or physiological conditions. Such a mechanism cannot be accepted as a functionally realistic one. In contrast to this, the parameter range is extensively broaden ed in our generalized scheme [note that $[2\beta-\alpha\gamma-2\sqrt{\beta(\beta-\alpha\gamma)}]/\gamma^2>0$ when $\beta-\alpha\gamma>0$, and see N in the left-hand side of the latter inequality in (3.31)]. In fact, a lot of synapses are formed on neuronal-cell membranes at high density, and therefore N is supposed to be very large in a real neuron. For such a large N, the switch mechanism is much more stabilized compared to that for $N=1$.

Note that we have used the terms ON and OFF in more generalized meanings compared to those used in the original Lisman model. In our generalized scheme, the state of the system is referred to as ON when one of the x_i's is positive, whereas the others are zero, and it is referred to as OFF when all of the x_i's are zero. Thus, there are N-mulitplicated ON states, and the process of synapse selection determines which of the ON states will be realized. For a help for understanding, the definitions of ON and OFF in our generalized scheme and those in the original Lisman model are illustrated in Table II. Thus, under the condition (3.31), the system in the generalized scheme functions not as a simple binary switch but as a hybridized one, i.e., a switch with the function of synapse selection.

In the analysis so far, we have postulated the following idealized situation: Transmission of a signal at each synapse takes place once, transiently, and simultaneously with those at the others, and x_i+y_i, which corresponds to the total of active- and inactive-enhancer concentrations in the ith spine, is constant with i at the initial time. That is, each synapse differs from the others only in the initial value of x_i (and thereby that of y_i because $x_i+y_i=\alpha$), and the other conditions for all synapses are equal at the initial time. This idealization has revealed novel properties of the interaction between synapses in

TABLE II. Definitions of ON and OFF states in our model and those in the original Lisman model. A solid or open circle in each box represents the state of a corresponding synapse: The ith circle is filled (●) if $x_i=v_{L_1}$, and it is opened (○) if $x_i=0$.

	The original Lisman model	Our model
ON	●	●○○···○○ ○●○···○○ ⋮ ○○○···○●
OFF	○	○○○···○○

our model: The order in the initial values of x_i's is the essential factor that determines the fate of each synapse. However, the above restriction might be relieved for considerations under more realistic situations. Therefore, we supposed that transmission of a signal at each synapse takes place repeatedly and asynchronously with those at the others, and numerically investigated how x_i's evolve with time. In this study, transmission of a signal at the ith synapse was represented by the term $z_i y_i$, which is added and subtracted from the right-hand sides of (2.20) and (2.21), respectively. Here, z_i is a function of s and defines the intensity of the signal transmitted at the ith synapse at time s; $z_i > 0$ if signal transmission at the ith synapse is active, and $z_i = 0$ if it is at rest. Figure 5 shows an example of results of numerical simulations for $N = 2$. The parameter values in this figure satisfy the condition (3.9) under which, as shown in Figs. 3(b) and 4, the system functions as a hybridized switch. At $s = 0$, $x_1 = x_2 = 0$ and $y_i = y_i = \alpha$. Just then, signal transmissions become active at both synapse 1 and synapse 2 with the different intensities such that $z_1 > z_2$ (P_1). After the termination of these signal transmissions, the difference between x_1 and x_2 is amplified and then x_1 converged to a positive value, whereas x_2 converges to zero; namely, synapse 1 is selected. Then, this is followed by a series of two signal transmissions at synapse 2. The intensity of the former signal transmission (P_2) is insufficient to make a new synapse selection, i.e., a selection of synapse 2. The intensity of the latter (P_3) is strong enough, so that the weight of synapse 2 is enhanced, and, instead, that of synapse 2 is reduced from the enhanced level to its basal one. Interestingly, a further signal transmission at synapse 1 (P_4) reduces the weight of synapse 2 to its basal level without enhancing that of synapse 1, namely the switch is turned OFF.

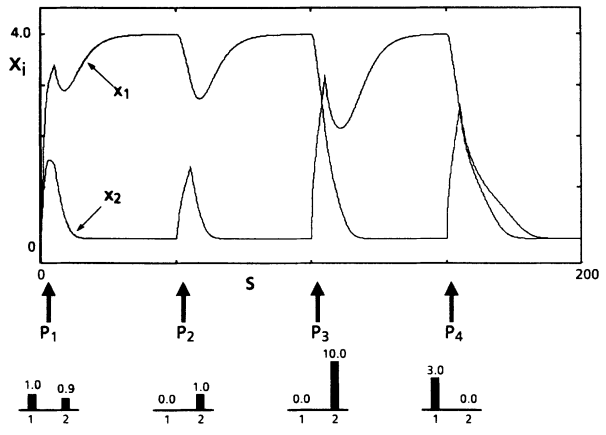

FIG. 5. Effects of signal transmissions at two neighboring synapses, each becomes active repeatedly and asynchronously to that at the other, on the synaptic-modification processes. The parameter values are set as the same as those for Fig. 3(b), and $(x_1, x_2)_{s=0} = (0.0, 0.0)$. The time courses of synaptic transmissions are set as follows: $(z_1, z_2) = (1.0, 0.9)$ $(0 \le s \le 5)$; $(z_1, z_2) = (0.0, 1.0)$ $(50 \le s \le 55)$; $(z_1, z_2) = (0.0, 10.0)$ $(100 \le s \le 105)$; $(z_1, z_2) = (3.0, 0.0)$ $(150 \le s \le 155)$; otherwise, $(z_1, z_2) = (0.0, 0.0)$. The arrows below the Figure indicate activations of signal transmissions, and the heights of the left and right bars below each arrow symbolize the intensities of signal transmissions at synapses 1 and 2, respectively.

IV. SUMMARY AND DISCUSSION

We have generalized the original Lisman model by taking solubilities of the enzymes into account, and discussed how synapses formed on the same neuron interact with one another through cytosolic transportation of the soluble enzyme between spines. Our model is described by a nonlinear dynamical system, and results of analytical and numerical investigations of this system have shown that it can be multistable and exhibit spontaneous symmetry breaking. This instability represents a competitive interaction between the modification processes at synapses, leading to a novel phenomenon which we have called "synapse selection": The weight of only one of the synapses, which is predominant at an initial time, is selectively enhanced at a thermal equilibrium limit and those at the others are returned to their basal levels in ascending order of their initial strengths. Moreover, a difficulty associated with the original Lisman model, i.e., that the parameter range in which the system functions as a switch is relatively narrow and accordingly the switch mechanism is functionally unstable against small changes in parameters, has been considerably improved by extensively broadening the parameter range. In this broadened parameter range, the system functions not as a simple binary switch but as a hybridized one, a switch with a single OFF state and multiple ON states; which of the ON states is realized is determined by the process of synapse selection.

It has not yet been experimentally confirmed whether a real neuron has a function such as synapse selection. However, it is not absurd to suppose that a real neuron has such a function, because synapse selection seems to be useful for feature grasping of a pattern. Consider a pattern consisting of several stimuli and let the index of the strongest stimulus and its intensity be the features of this pattern. A neuron that performs synapse selection can extract the features of a given pattern and store them.

As shown in Fig. 5, a memory stored in the system is alterable. At the first stage in Fig. 5, the system stores the features of the first pattern (P_1 in Fig. 5). Next, the system then receives the second pattern (P_2), but it still retains the old memory because the features of the second pattern are not so prominent. However, those of the third one (P_3) are so prominent that the system forgets the old memory and newly stores the features of the third pattern.

The analyses of our model have been performed under the steady-state assumptions for intermediary metabolites, (2.11) and (2.12). However, the mathematical scheme that "exactly" describes our model is given not by the equations that we have dealt with but by (2.4)–(2.10). Hence, there arises a question: Are the novel properties obtained in our analyses, such as synapse selection, or hybrid switching, essential features of our model, or merely side effects of the steady-state assumptions? Indeed, equilibrium points of the system in the exact scheme are the same as those of that in the simplified

scheme, but it is not so easy to determine their stabilities in an analytical way because the exact scheme contains so many independent variables and parameters. Therefore, we investigated the dynamical structure of the exact scheme by numerically calculating its time evolution for various sets of parameter values and initial conditions for variables. Results of the investigation indicate that the classification of the structures of the simplified scheme, discussed in detail in Sec. III, is almost valid also in the exact scheme (data not shown), suggesting that the essential features of the model are not spoiled by the steady-state assumptions for intermediary metabolites.

In this paper we have postulated that the enhancer in the inactive form is soluble, whereas the enhancer and the inactivator in the other forms are membrane associated. However, there are several other possibilities. Indeed, very little is known about enzymes responsible for synaptic enhancement, including their names, their solubilities, etc.; thus, we have nowadays no experimental evidence to exclude these other possibilities that we have not entered in the present study. Some of them, however, can be ruled out by the following speculations: First, it is natural to suppose that E^*E is membrane associated if E^* or E is membrane associated; otherwise, it is soluble. IE^* is membrane associated if I or E^* is membrane associated; otherwise, it is soluble. Second, E^* is supposed to be insoluble from the following consideration: If it is soluble, flow flux for E^*,

$$J_{E^*_{ij}}\left[=-\frac{D_{E^*}V([E^*]_i-[E^*]_j)}{Sd}\right],$$

will tend to vanish as $t\to\infty$, giving

$$[E^*]_1=[E^*]_2=\cdots=[E^*]_N$$

at a thermal equilibrium limit. In this limit, the weight of each synapse is equal to those of the others; in other words, each synapse completely loses its use-dependent specificity. Therefore, if learning and memory processes in the real brain are performed by use-dependent specific changes in synaptic weights, it is unlikely that E^* is soluble. Third, if E, E^*, and I are all membrane associated, there is no enzyme transportation between spines, resulting in no interactions between synapses. Such a scheme is nothing but the original one discussed by Lisman. On the basis of these speculations, two possible cases still remain to be examined: (1) E and I are soluble, whereas E^* is membrane associated, and (2) I is soluble, whereas E and E^* are membrane associated. Studies for these cases are now in progress and results of them will be reported in forthcoming papers.

In the present study the model has been discussed without specifying the names of the enzymes. In fact, little is experimentally established about enzymes responsible for synaptic modification. However, physiological and biochemical studies on long-term synaptic potentiation (LTP) in rat hippocampus [3], an experimental model for learning and memory in mammalian brains, suggest that the activities of protein kinases contribute to synaptic enhancement. Protein kinases are enzymes that catalyze phosphorylations of substrate proteins, and among them, Ca^{2+}/phospholipid-dependent protein kinase (PKC) is considered to play an important role in LTP. It may be worthwhile to mention that PKC shows similar biochemical properties to those postulated for the enhancer in the present study; inactive PKC is soluble in cytosol, whereas it translocates to membrane and becomes active associating to LTP [9].

The present study proposes a pattern-encoding rule based on synapse selection, strongly suggesting that molecular and cellular levels of consideration must be included for exploration of network levels of information processing in the brain. It will be an interesting work to investigate the performance of neural networks that obey such a pattern-encoding rule.

[1] T. H. Brown, E. W. Kairiss, and C. L. Keenan, Annu. Rev. Neurosci. **13**, 475 (1990), and references therein.
[2] J. E. Lisman, Proc. Natl. Acad. Sci. USA **82**, 3055 (1985).
[3] T. V. P. Bliss and G. L. Collingridge, Nature **361**, 31 (1993), and references therein.
[4] C. Koch and A. Zador, J. Neurosci. **13**, 413 (1993).
[5] H. Okamoto and K. Ichikawa, *Proceedings of the International Joint Conference on Neural Networks '93 NAGOYA* (IEEE, New York, 1993), pp. 101–104.
[6] A similar mathematical scheme for a reaction-diffusion system is used in A. Hjelmfelt, F. W. Schneider, and J. Ross, Science **260**, 335 (1993).
[7] See, for example, D. Voet and J. G. Voet, Biochemistry (Wiley, New York, 1990).
[8] See, for example, J. Guckenheimer and P. J. Holmes, *Nonlinear Oscillations, Dynamical Systems, and Bifuractions of Vector Fields* (Springer-Verlag, New York, 1983).
[9] R. F. Akers, D. M. Lovinger, P. A. Colley, D. J. Linden, and A. Routtenberg, Science **231**, 587 (1986).

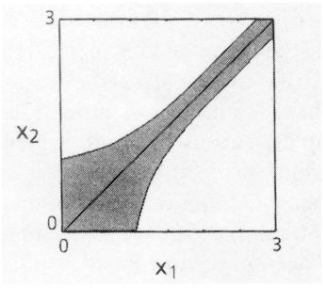

FIG. 4. Relation between $(x_1,x_2)_{s=0}$ and the final state of the switch. The parameter values were set as the same as those for Fig. 3(b). If (x_1,x_2) starts from the shaded region, then the switch is turned OFF; if it starts from either of the open regions, then the switch is turned ON.